

Research Article

Effect of Molecular Chain Structure on Fracture Mechanical Properties of Aeronautical Polymethyl Methacrylate Using Extended Digital Image Correlation Method

Wei Shang,¹ Xiaojing Yang,² Xinhua Ji,³ and Zhongxian Liu¹

¹Key Laboratory of Protection and Retrofitting for Civil Building and Construction of Tianjin, Tianjin Chengjian University, Tianjin 300384, China

²School of Materials Science and Engineering, Hebei University of Technology, Tianjin 300130, China

³Department of Mechanics, Tianjin University, Tianjin 300072, China

Correspondence should be addressed to Wei Shang; wshang@tju.edu.cn and Xiaojing Yang; yxjing@mail.nankai.edu.cn

Received 4 January 2016; Revised 18 May 2016; Accepted 29 May 2016

Academic Editor: Luciano Lamberti

Copyright © 2016 Wei Shang et al. This is an open access article distributed under the Creative Commons Attribution License, which permits unrestricted use, distribution, and reproduction in any medium, provided the original work is properly cited.

The main purpose of this work is to investigate the fracture mechanical properties of aeronautical polymethyl methacrylate, which has been treated with directional tensile technology. Because of the special processing of directional polymethyl methacrylate, the molecular chain structures are different in different directions. The mechanical properties depend on the specific molecular chain structures. We use extended digital image correlation to measure the displacement field near the tip of the crack when the cracks grow in different directions in directional polymethyl methacrylate. We then tested the critical load for different specimens and analyzed the fracture morphology of the different specimens. Thanks to the experimental results, a molecular chain model of directional polymethyl methacrylate could be established. The analysis results using the molecular chain model are consistent with the experiments, which confirms the reliability of the molecular chain model.

1. Introduction

Polymethyl methacrylate (PMMA) is widely used in the field of aviation, due to its excellent properties, such as lightweight, high temperature resistance, high light transmittance, and good mechanical properties. The mechanical properties of PMMA have attracted additional attention after several plane crashes were caused by cracks in a hatch made of PMMA.

Research on fatigue and fracture properties of polymer materials started in the 1960s because of high requirements for strength and reliability. Berry [1] confirmed that Griffith strength theory could be used to analyze the brittle fracture of PMMA. Recently, this theory and related experiments have become important means to analyze the fracture of polymer material in general. Mukherjee and Burns [2] proposed that fatigue of PMMA was determined by three parameters: stress intensity factor amplitude, average stress intensity factor, and frequency. Woo and Chow [3] unified the fatigue crack propagation formula for metal aluminum and the nonmetallic

PMMA. They proposed that the strain energy release rate amplitude should be used to analyze crack propagation but not the stress intensity factor amplitude. Cheng et al. [4, 5] studied the influence of temperature and loading rate on the tensile strength and fracture toughness of PMMA. Kim et al. [6, 7] proposed that the fatigue crack growth rate of most polymers increases with increasing temperature and decreases with increasing loading frequency. Ramsteiner and Armbrust [8] solved some fatigue practical problems with polymers, such as the measurement of crack propagation, the influence of the specimen shape, the applied frequency, the measurement with constant or increasing stress intensity amplitude, and the propagating crack as a signal for transitions in the internal deformation process. Yao et al. [9] investigated the dynamic fracture behavior of thin PMMA plates with three- and four-parallel edge cracks using the method of caustics and a high-speed Schardin camera. Yao et al. [10] investigated dynamic fracture behavior of a thin PMMA sheet with two overlapping offset-parallel cracks

under tensile loading using the optical method of caustics in combination with a Cranz-Schardin high-speed camera. Xu et al. also [11] studied the fracture characterization of a V-notch tip in PMMA material using an optical caustics method. Sahraoui et al. [12] measured the dynamic fracture toughness of notched PMMA at high impact velocities, where the classical method is limited by the inertial effects. The direct measurements of the specimen deflection are successfully used for toughness evaluation. Zhang et al. [13] studied the fracture characteristics of PMMA with different offset cracks under three-point bending using the digital gradient sensing method. Ayatollahi et al. [14] studied the brittle fracture characteristics of PMMA under compressive loading using the theoretical and experimental methods. Berto et al. [15, 16] studied the fracture characteristics of PMMA using notched specimens tested under torsion at room temperature and at -60 degrees C.

Sauer and Hsiao began to investigate the craze phenomenon of polymers in 1949. Kies and his coworkers were inspired because the top of PMMA hatch has improved craze resistance. They studied biaxial and multiaxial tension oriented PMMA. Oriented PMMA is manufactured as follows: a PMMA plate is pulled under directional stresses following a preselected temperature profile that includes heating, keeping, and cooling. Oriented PMMA has a higher pull strength and elasticity module than normal PMMA. Some important components (e.g., hatches) of airplanes are often made of oriented PMMA plates.

There have been extensive studies of the mechanical properties of PMMA. However, most of the previous studies use the isotropic mechanical model. Because of the special processing of oriented PMMA, the molecular chain structures vary in different directions. The fracture mechanical properties depend on the molecular chain structures. Therefore, the isotropic mechanical model is unable to describe the mechanical properties of oriented PMMA [17].

Extended digital image correlation was used to measure the displacement field near the tip of the crack when cracks grow in different directions. In addition, the critical load for different samples was tested. The fracture morphology represents the historical record of the material fracture. The mechanism of the fracture can be found via analysis of the fracture morphology. The fracture morphology of different specimens was also analyzed. Based on the experimental results, the molecular chain model of oriented PMMA was established. The molecular chain model can be used to analyze the fracture mechanical properties of oriented PMMA. The analysis results of the molecular chain model are consistent with the experimental results, which also confirm the reliability of the molecular chain model.

2. Extended Digital Image Correlation

Digital image correlation (DIC) [18–20] is an established method to measure mechanical parameters. However, this method is not applicable for displacement measurement of a discontinuous interface and cannot solve fracture problems. Recently, an algorithm named extended digital image correlation (X-DIC) [21–25] has been used to solve this problem. The

method tracks the gray value pattern in small neighborhoods called subsets during deformation. Two digital images (the reference image and the deformed image) are used to record the surface changes of the specimen. Here, $f(x, y)$ is the gray level value at coordinate (x, y) of the reference image, and $g(x^*, y^*)$ is the gray level value at coordinate (x^*, y^*) of the deformed image. Any point with coordinates (x, y) in the reference image relates to the deformed image via the deformation

$$\begin{aligned} x^* &= x + u \\ y^* &= y + v. \end{aligned} \quad (1)$$

In this equation, u and v are the horizontal and vertical displacements of the point (x, y) , respectively.

According to the gray level values of the reference image and the deformed image, the correlation factor is expressed as

$$S = 1 - \frac{\sum f(x, y) \cdot g(x + u^{\text{test}}, y + v^{\text{test}})}{\sqrt{\sum f^2(x, y) \cdot \sum g^2(x + u^{\text{test}}, y + v^{\text{test}})}}. \quad (2)$$

In (2), when the correlation factor S has the minimum value, the real displacement is $u = u^{\text{test}}$ and $v = v^{\text{test}}$.

In this step, a correlation algorithm that is directly linked with finite element simulations is developed. We chose the Bilinear Quadrilateral (Q4) finite elements as the simplest basis. The element is considered a subset of the correlation algorithm. Within the subset, the displacement field is [26]

$$\begin{aligned} \vec{u}(\vec{x}) &= \sum_{I \in K} N_I(\vec{x}) \left[\vec{a}_I + \frac{H(\vec{x})}{I \in K_T} \vec{b}_I + \sum_{l=1}^4 \underbrace{B_I^l(\vec{x})}_{I \in K_\Lambda} \vec{c}_I^l \right]. \end{aligned} \quad (3)$$

In (3), $\vec{u}(\vec{x})$ is the displacement vector; N_I is the Q4 shape function; \vec{a}_I are the displacement components of the nodes; \vec{b}_I are the improved degrees of freedom of the nodes on the unit cut by the crack; \vec{c}_I^l are the improved degree of freedom of the nodes on the unit that includes the tip of the crack; K is the set of all nodes; K_T is the set of nodes cut by crack; K_Λ is the set of nodes on the unit that includes the tip of the crack; $H(\vec{x})$ is called Heaviside Function and expressed as

$$H(\vec{x}) = \begin{cases} 1 & \text{if } (x - x^*) \cdot n > 0, \\ -1 & \text{otherwise,} \end{cases} \quad (4)$$

where x is the sample point, x^* is the closest point to x that lies on the crack, and n is the direction vector perpendicular to the crack face at x^* . $B_I^l(\vec{x})$ is the function of the tip of the crack and expressed in the local coordinate system as follows:

$$\begin{aligned} [B_I^l(r, \theta)] &= \left[\sqrt{r} \sin\left(\frac{\theta}{2}\right), \sqrt{r} \cos\left(\frac{\theta}{2}\right), \sqrt{r} \sin\left(\frac{\theta}{2}\right) \right. \\ &\quad \left. \cdot \sin(\theta), \sqrt{r} \cos\left(\frac{\theta}{2}\right) \sin(\theta) \right]. \end{aligned} \quad (5)$$

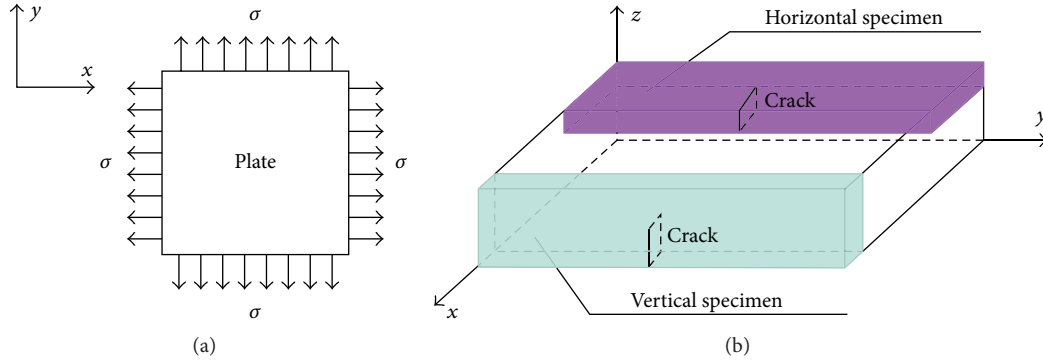


FIGURE 1: Two types of specimens: (a) biaxial tension PMMA plate; (b) two specimens in different directions.

r and θ are the polar coordinates in the local tip of the crack coordinate system.

3. Experiment and Analysis

3.1. Displacement Near the Tip of the Crack. In order to investigate the mechanical properties in different directions of the oriented PMMA plate, two specimens were cut from an oriented PMMA plate in different directions shown in Figure 1. Pulling loads during the process are in x - y plane.

The fracture mechanical properties of oriented PMMA are studied with the three-point bending beams shown in Figure 2. The length of the horizontal specimen is 120 mm; the width is 30 mm; the crack length is 14 mm. The crack direction is x , which is also the oriented direction. The length of the vertical specimen is 30 mm; the width is 7.5 mm; the crack length is 2.2 mm. The crack direction is z , which is perpendicular to the oriented direction.

Usually the front of a crack is subjected to three-dimensional effects that should be considered. Three-dimensional effects near the front were subjected to many analytical, numerical, and experimental studies in the past 50 years [27–29]. In this paper, the direction of crack propagation is studied using the displacement field of the tip of the crack. The three-dimensional effects do not affect the conclusions of this paper. Extended digital image correlation was used to test the displacement field near the tip of the crack of specimens. Considering the experimental results, the fracture mechanical properties of oriented PMMA were analyzed. The surfaces of both the horizontal and vertical specimen have the prefabricated spot shown in Figures 3(a) and 3(c). According to the surface images of loads 355 N and 817 N, extended digital image correlation was used to measure the y direction displacement field near the tip of the crack of the horizontal specimen shown in Figure 3(b). In addition, according to the surface images of loads 114 N

and 187 N, extended digital image correlation is also used to measure the displacement field in y direction near the tip of the crack of the vertical specimen shown in Figure 3(d). The displacement field in y direction near the tip of the crack of the horizontal specimen is symmetrical. Therefore, the crack of the horizontal specimen grows in the crack direction, while the displacement field in y direction near the tip of the crack of the vertical specimen is not symmetric. The crack of the vertical specimen grew in an oblique direction.

The crack propagation directions of different specimens were analyzed. The maximum circumferential normal stress theory is a type of crack propagation criterion. When the circumferential normal stress reaches the limit values, the crack begins to grow. This crack propagation criterion is the simplest and often used. According to maximum circumferential normal stress theory, the crack of the three-point bending beam grows in the crack direction. The experiments show that the crack of the horizontal specimen grows in the crack direction. Therefore, maximum circumferential normal stress theory is consistent with our experimental results. However, the theory is not suitable to be applied to the vertical specimen. The crack of the vertical specimen grows in an oblique direction. The reason will be analyzed. Because the molecular chains vertical to the oriented direction are not oriented, the mechanical properties are inferior compared with the oriented direction. The nonoriented molecular chains of the vertical specimen are damaged first, so the crack of the vertical specimen grows in an oblique direction.

3.2. Critical Load. Fracture toughness is important for the fracture mechanical properties of oriented PMMA. Fracture toughness is tested in two directions for the horizontal and the vertical specimen [13]. One is in the direction of the directional tension; the other is perpendicular to it. Equation (6) is the formula for the stress intensity factor.

$$K_I = \frac{PS}{BW^{3/2}} f\left(\frac{a}{W}\right) \quad (6)$$

$$f\left(\frac{a}{W}\right) = \frac{3(a/W)^{1/2} [1.99 - (a/W)(1 - a/W)(2.15 - 3.93(a/W) - 2.7(a^2/W^2))]}{2(1 + 2a/W)(1 - a/W)^{3/2}}, \quad (7)$$

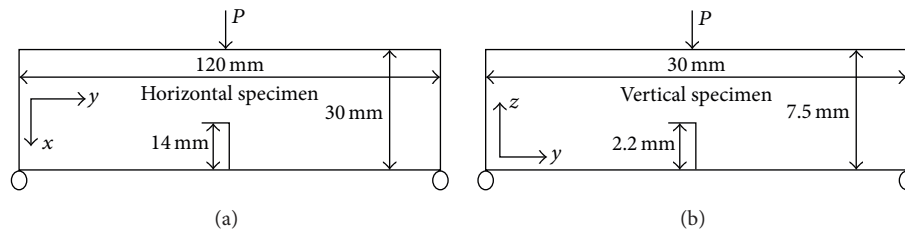


FIGURE 2: Dimensions of the three-point bending beams: (a) horizontal specimen; (b) vertical specimen.

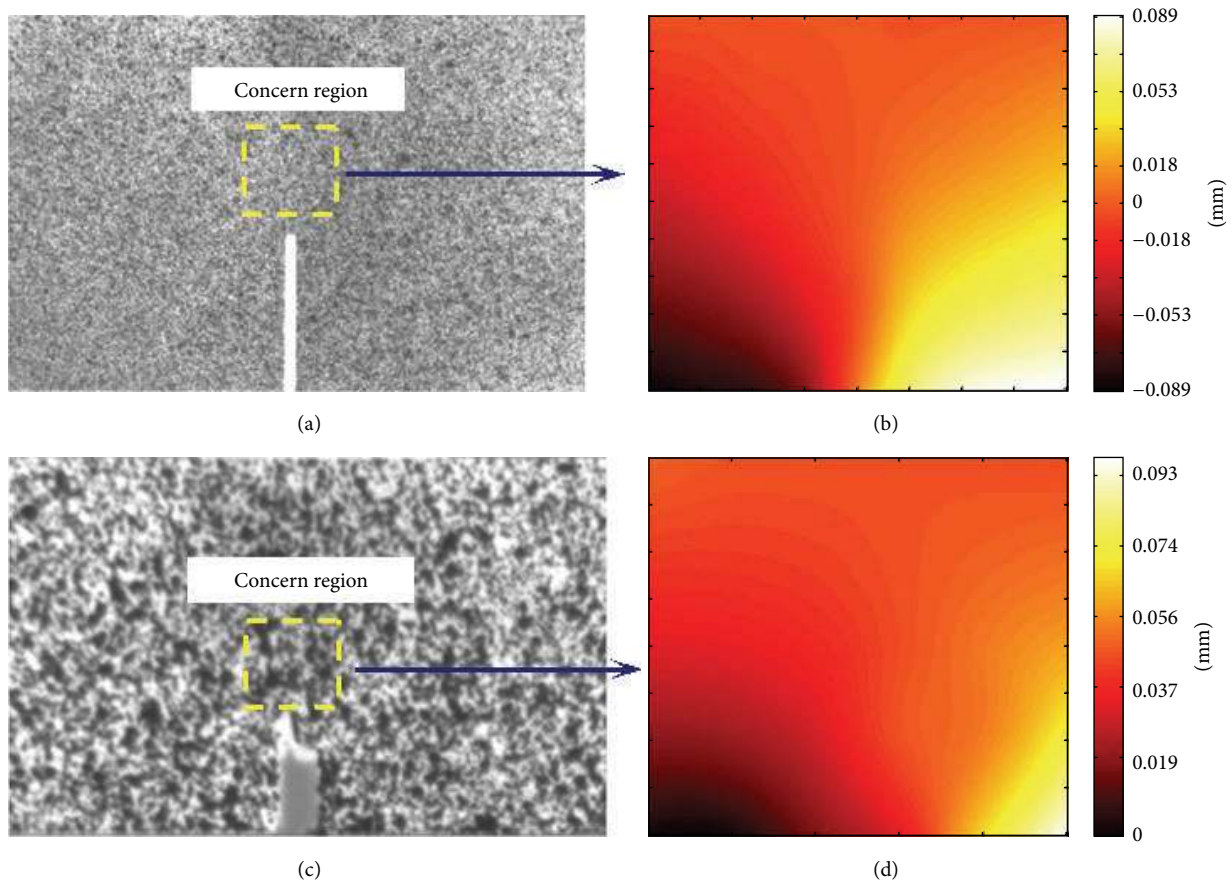


FIGURE 3: Experimental results: (a) gray image of the horizontal specimen; (b) y direction field of the horizontal specimen; (c) gray image of vertical specimen; (d) y direction displacement field of the vertical specimen.

where B is the thickness, $W = 2B$ is the width, $S = 4W$ is the length, a is the length of crack, and P is the load.

The length of the horizontal specimen is 120 mm; the width is 30 mm; the crack length is 14 mm. The crack direction is in the oriented direction. The length of the vertical specimen is 30 mm; the width is 7.5 mm; the crack length is 2.2 mm.

The goal of fracture toughness testing is to find the critical load for crack propagation using P - V curve. Load P was tested with a load sensor, and the crack opening displacement V was tested using the extensometer normally. The specimen is very small, so there is not enough space to attach the extensometer. Hence, digital image correlation, which

replaces the extensometer, is applied to the test crack opening mouth displacement V . The tester and digital CCD camera are synchronous, so CCD could collect speckle patterns of different loads, which were used to draw P - V curve shown in Figure 4.

The critical load of the horizontal specimen was 817 N. The fracture toughness value was $194.87 \text{ N/mm}^{3/2}$ for the horizontal specimen which was obtained using the critical load and specimen size using (6). The critical load of the vertical specimen was 208 N. Similarly, the fracture toughness value $91.32 \text{ N/mm}^{3/2}$ of the vertical specimen was obtained. Due to the restrictions of the plate thickness, the vertical specimen is small and the sizes of horizontal and vertical

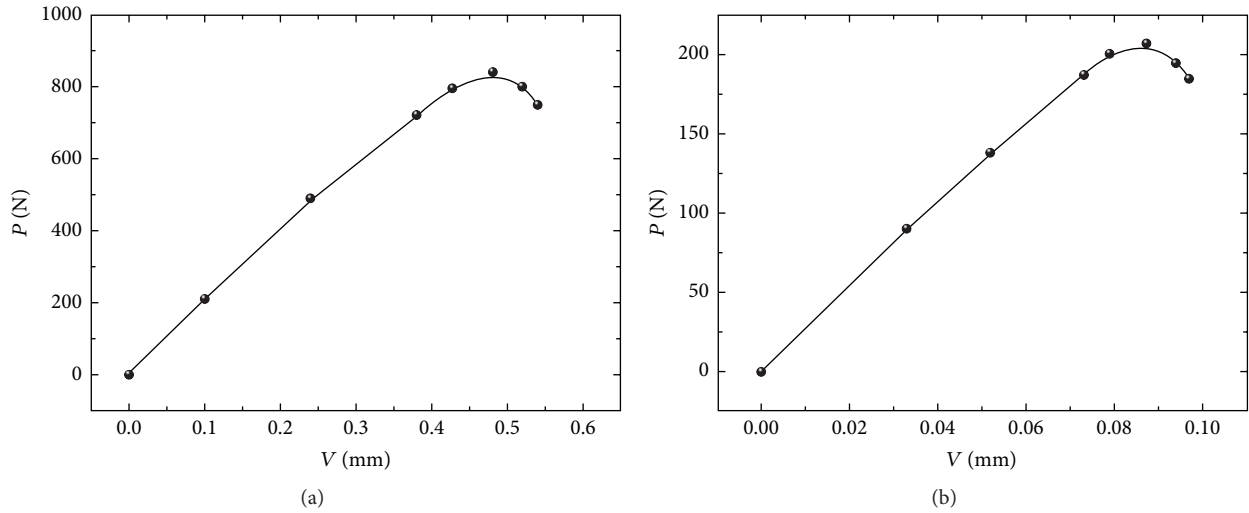


FIGURE 4: P - V curves: (a) horizontal specimen; (b) vertical specimen.

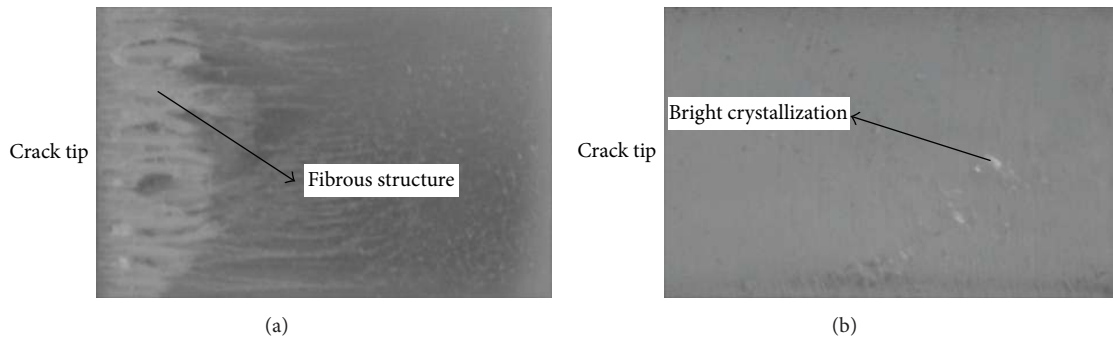


FIGURE 5: Macroscopic fracture morphology: (a) fracture morphology of the horizontal specimen; (b) fracture morphology of the vertical specimen.

TABLE 1: Critical loads for different specimens.

Specimens	Horizontal specimen	Vertical specimen
Critical load (N)	817	383

specimens are different. In this paper, the fracture toughness is used to calculate the critical loads of the same size, which can reflect the fracture mechanical properties in different directions clearly. Considering (6), if the vertical specimen is as big as the horizontal specimen, the critical load is 383 N shown in Table 1. The experimental results show that the critical load of the horizontal specimen is larger than that of the vertical one. Hence, the crack perpendicular to the directional tension grows more easily.

3.3. Fracture Morphology. The fracture morphology is a record of the material fracture. The analysis of the fracture morphology is used to analyze the fracture process according to the observation and analysis of the macroscopic and microscopic characteristics. The mechanism of the fracture can be found via analysis of the fracture morphology. The fracture morphology of both the horizontal and the vertical

specimen is shown in Figures 5(a) and 5(b). The fracture surface of the horizontal specimen has a fibrous structure, suggesting a ductile fracture. The fracture surface of the horizontal specimen shows clear plastic deformation, while the fracture surface of the vertical specimen shows no plastic deformation but reveals bright crystallization indicating a brittle fracture. Based on the analysis of the fracture morphology we conclude that the horizontal specimen has superior fracture mechanical properties compared to the vertical specimen because of the oriented molecular chains.

4. Molecular Chain Model

The crack propagation direction of the horizontal and vertical specimen is shown in Figures 6(a) and 6(c). Because the molecular chains in x and y directions are oriented, the mechanical properties are enhanced. The molecular chains in x and y directions are represented by thick solid lines in Figures 6(b) and 6(d). Because the molecular chains in z direction are not oriented, the mechanical properties are weak compared with x and y directions. The molecular chains in z direction are represented using thin dotted lines in Figure 6(d).

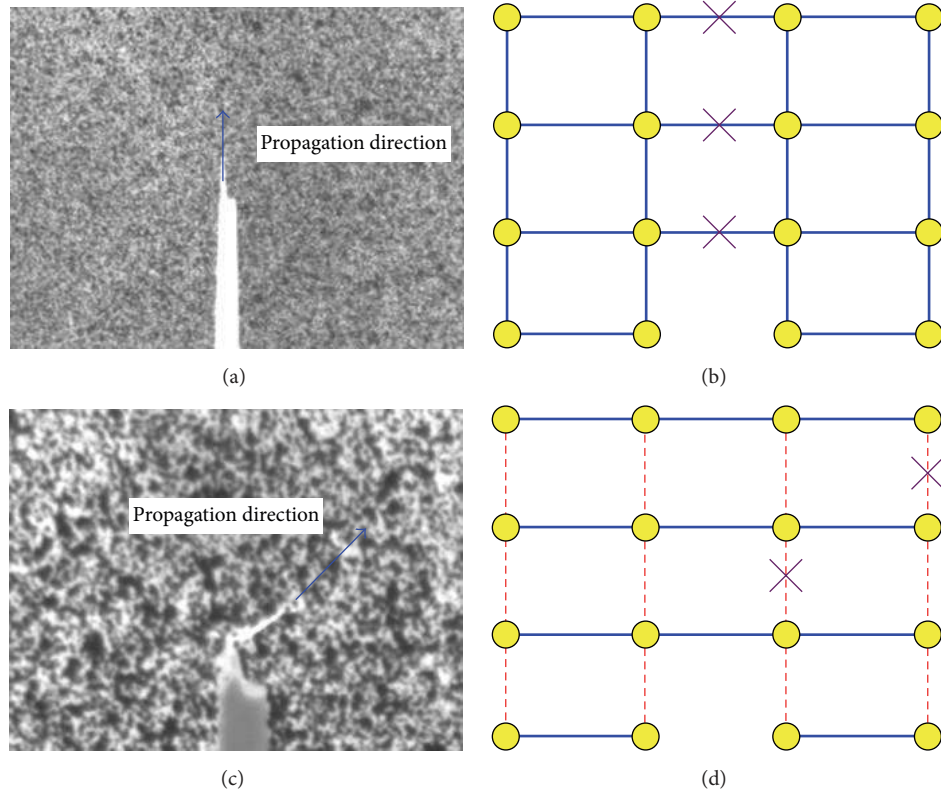


FIGURE 6: Crack propagation direction: (a) propagation direction of the horizontal specimen; (b) propagation direction schematic of the horizontal specimen; (c) propagation direction of the vertical specimen; (d) propagation direction schematic of the vertical specimen.

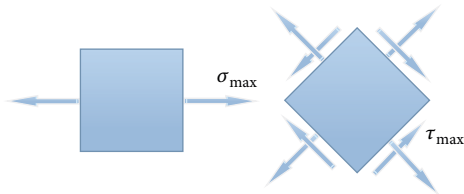


FIGURE 7: Stress state of the tip of the crack.

For the horizontal specimen, when the maximum tensile stress is equal to the value of the tensile strength shown in Figure 7, the crack begins to grow. Because of the large tensile stress, the molecular chains of the tip of the crack are damaged. They are represented by \times symbol in Figure 6(b). The crack of the horizontal specimen grows in crack direction, while the nonoriented molecular chains of the vertical specimen are weak. When the maximum shear stress of the tip of the crack equals the shear strength shown in Figure 7, the molecular chains in vertical direction represent the shear failure indicated by \times symbol in Figure 6(d). The direction of the maximum shear stress occurs at a 45-degree angle shown in Figure 7. Hence, the crack of the vertical specimen grows at 45 degrees. The conclusions based on the molecular chain model are consistent with the experimental results.

5. Conclusion

Extended digital image correlation was used to measure the displacement field near the tip of the crack when the cracks grow in different directions in oriented PMMA. The crack of the horizontal specimen grows in the crack direction, while the crack of the vertical specimen grows in an oblique direction. Because the molecular chains perpendicular to the oriented direction are not oriented, the mechanical properties are weaker. The nonoriented molecular chains of the vertical specimen are damaged first, and the crack grows in an oblique direction.

The critical load of different specimens was measured. The experiment shows that the critical load of the horizontal specimen is larger than that of the vertical specimens. Therefore, the crack perpendicular to the directional tension grows more easily.

Based on the analysis of the fracture morphology we conclude that the horizontal specimen has better fracture mechanical properties than the vertical specimen because of the oriented molecular chains.

Based on our experiments, the molecular chain model of oriented PMMA could be established. The analysis results using the molecular chain model are consistent with the results of the experiment, which confirms the reliability of the molecular chain model. Using the molecular chain model, the surface crack of the real component should be paid more

attention to because the crack in the thickness direction grows more easily.

Competing Interests

The authors declare that there are no competing interests regarding the publication of this article and regarding the funding that they have received.

Acknowledgments

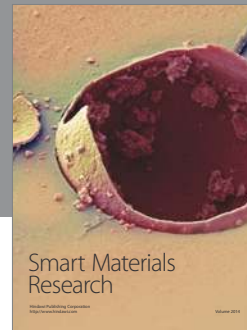
The authors acknowledge the financial support of the National Natural Science Foundation of China (Grants nos. 11402166, 51301057, 51208336, and 51408400) and the General Projects in Tianjin Research Program of Application Foundation and Advanced Technology (Grants nos. 13JCYBJC39100 and 14JCYBJC21900).

References

- [1] J. P. Berry, "Fracture processes in polymeric materials. I. The surface energy of poly(methyl methacrylate)," *Journal of Polymer Science*, vol. 50, no. 153, pp. 107–115, 1961.
- [2] B. Mukherjee and D. J. Burns, "Fatigue-crack growth in polymethylmethacrylate," *Experimental Mechanics*, vol. 11, no. 10, pp. 433–439, 1971.
- [3] C. W. Woo and C. L. Chow, "Fatigue crack propagation in aluminium and PMMA," *International Journal of Fracture*, vol. 26, no. 2, pp. R37–R42, 1984.
- [4] W. M. Cheng, G. A. Miller, J. A. Manson, R. W. Hertzberg, and L. H. Sperling, "Mechanical behaviour of poly(methyl methacrylate)—part 1 Tensile strength and fracture toughness," *Journal of Materials Science*, vol. 25, no. 4, pp. 1917–1923, 1990.
- [5] W. M. Cheng, G. A. Miller, J. A. Manson, R. W. Hertzberg, and L. H. Sperling, "Mechanical behaviour of poly (methyl methacrylate). Part 2 the temperature and frequency effects on the fatigue crack propagation behaviour," *Journal of Materials Science*, vol. 25, no. 4, pp. 1924–1930, 1990.
- [6] H.-S. Kim and Y.-W. Mai, "Effect of temperature on fatigue crack growth in unplasticized polyvinyl chloride," *Journal of Materials Science*, vol. 28, no. 20, pp. 5479–5485, 1993.
- [7] H. S. Kim and X. M. Wang, "Temperature and frequency effects on fatigue crack growth of UPVC," *Journal of Materials Science*, vol. 29, no. 12, pp. 3209–3214, 1994.
- [8] F. Ramsteiner and T. Armbrust, "Fatigue crack growth in polymers," *Polymer Testing*, vol. 20, no. 3, pp. 321–327, 2001.
- [9] X. F. Yao, G. C. Jin, K. Arakawa, and K. Takahashi, "Experimental studies on dynamic fracture behavior of thin plates with parallel single edge cracks," *Polymer Testing*, vol. 21, no. 8, pp. 933–940, 2002.
- [10] X. F. Yao, W. Xu, M. Q. Xu, K. Arakawa, T. Mada, and K. Takahashi, "Experimental study of dynamic fracture behavior of PMMA with overlapping offset-parallel cracks," *Polymer Testing*, vol. 22, no. 6, pp. 663–670, 2003.
- [11] W. Xu, X. F. Yao, M. Q. Xu, G. C. Jin, and H. Y. Yeh, "Fracture characterizations of V-notch tip in PMMA polymer material," *Polymer Testing*, vol. 23, no. 5, pp. 509–515, 2004.
- [12] S. Sahraoui, A. El Mahi, and B. Castagnède, "Measurement of the dynamic fracture toughness with notched PMMA specimen under impact loading," *Polymer Testing*, vol. 28, no. 7, pp. 780–783, 2009.
- [13] R. Zhang, R. Guo, and S. Wang, "Mixed mode fracture study of PMMA using digital gradient sensing method," *Engineering Fracture Mechanics*, vol. 119, pp. 164–172, 2014.
- [14] M. R. Ayatollahi, A. R. Torabi, and M. Firoozabadi, "Theoretical and experimental investigation of brittle fracture in V-notched PMMA specimens under compressive loading," *Engineering Fracture Mechanics*, vol. 135, pp. 187–205, 2015.
- [15] F. Berto, D. A. Cendon, P. Lazzarin, and M. Elices, "Fracture behaviour of notched round bars made of PMMA subjected to torsion at -60°C ," *Engineering Fracture Mechanics*, vol. 102, pp. 271–287, 2013.
- [16] F. Berto, M. Elices, P. Lazzarin, and M. Zappalorto, "Fracture behaviour of notched round bars made of PMMA subjected to torsion at room temperature," *Engineering Fracture Mechanics*, vol. 90, pp. 143–160, 2012.
- [17] W. Shang, X. J. Yang, and L. N. Zhang, "Study of anisotropic mechanical properties for aeronautical PMMA," *Latin American Journal of Solids and Structures*, vol. 11, no. 10, pp. 1777–1790, 2014.
- [18] W. H. Peters and W. F. Ranson, "Digital imaging techniques in experimental stress analysis," *Optical Engineering*, vol. 21, no. 3, pp. 427–431, 1982.
- [19] L. C. S. Nunes and J. M. L. Reis, "Experimental investigation of mixed-mode-I/II fracture in polymer mortars using digital image correlation method," *Latin American Journal of Solids and Structures*, vol. 11, no. 2, pp. 330–343, 2014.
- [20] B. Pan, L. Yu, and D. Wu, "Accurate ex situ deformation measurement using an ultra-stable two-dimensional digital image correlation system," *Applied Optics*, vol. 53, no. 19, pp. 4216–4227, 2014.
- [21] G. Besnard, F. Hild, and S. Roux, "'Finite-element' displacement fields analysis from digital images: application to Portevin-Le Châtelier bands," *Experimental Mechanics*, vol. 46, no. 6, pp. 789–803, 2006.
- [22] J. Réthoré, F. Hild, and S. Roux, "Extended digital image correlation with crack shape optimization," *International Journal for Numerical Methods in Engineering*, vol. 73, no. 2, pp. 248–272, 2008.
- [23] S. Roux and F. Hild, "Digital image mechanical identification (DIMI)," *Experimental Mechanics*, vol. 48, no. 4, pp. 495–508, 2008.
- [24] X. C. Zhang, G. Yang, N. Zhan, and H. Ji, "Gray change detection method for damage monitoring in materials," *Applied Optics*, vol. 54, no. 4, pp. 934–939, 2015.
- [25] J. L. Chen, N. Zhan, X. C. Zhang, and J. X. Wang, "Improved extended digital image correlation for crack tip deformation measurement," *Optics and Lasers in Engineering*, vol. 65, pp. 103–109, 2015.
- [26] N. Moës, J. Dolbow, and T. Belytschko, "A finite element method for crack growth without remeshing," *International Journal for Numerical Methods in Engineering*, vol. 46, no. 1, pp. 131–150, 1999.
- [27] Z. He, A. Kotousov, A. Fanciulli, F. Berto, and G. Nguyen, "On the evaluation of stress intensity factor from displacement field

affected by 3D corner singularity," *International Journal of Solids and Structures*, vol. 78-79, pp. 131-137, 2016.

- [28] A. Kotousov, Z. He, and A. Fanciulli, "Application of digital image correlation technique for investigation of the displacement and strain fields within a sharp notch," *Theoretical and Applied Fracture Mechanics*, vol. 79, pp. 51-57, 2015.
- [29] L. P. Pook, "A 50-year retrospective review of three-dimensional effects at cracks and sharp notches," *Fatigue & Fracture of Engineering Materials & Structures*, vol. 36, no. 8, pp. 699-723, 2013.



Hindawi

Submit your manuscripts at
<http://www.hindawi.com>

